

# Förster Resonance Energy Transfer Sensitized Singlet Fission in BODIPY-Pentacene Dimer Conjugates

Anna-Sophie Wollny, Giulia Lavarda, Ilias Papadopoulos, Ismael López-Duarte, Henrik Gotfredsen, Yuxuan Hou, Rik R. Tykwinski,\* Tomás Torres,\* and Dirk M. Guldi\*

In the present work, the energy donor 4,4-difluoro-4-bora-3a,4a-diaza-s-indacene (BODIPY) is used for the first time in combination with a pentacene dimer (Pnc<sub>2</sub>) to provide the conjugate BODIPYPnc<sub>2</sub> that features absorption throughout a large part of the solar spectrum. Upon photoexcitation, the singlet excited state energy of BODIPY is transferred to the pentacene dimer via intramolecular Förster resonance energy transfer (FRET). Subsequently, the pentacene dimer undergoes intramolecular singlet fission. In this process, a singlet correlated triplet pair is generated from the first singlet excited state via coupling to an intermediate state. The results show that solvent polarity has an influence on the system, with the largest FRET rate (i.e.,  $7.46 \times 10^{11} \text{ s}^{-1}$ ) being obtained in the most polar solvent (namely, benzonitrile) along with the largest triplet quantum yield (i.e.,  $207 \pm 20\%$ ).

## 1. Introduction

Solar cells are considered one of the most promising approaches to overcome the looming energy crisis.<sup>[1]</sup> Single-junction architectures, however, feature a thermodynamic limit of 32% which restricts their efficiencies. A convenient strategy to surpass this limit is through singlet fission (SF),<sup>[2]</sup> which can boost solar-to-electricity conversion efficiencies up to 44%.<sup>[3]</sup> In this spin-allowed process, a chromophore in the excited state shares its energy with a ground-state neighboring chromophore, which results in two separated triplet excited states with lower energy. Thus, two excited states are, in principle, produced from one photon.

For SF to occur, several criteria must be met. Two energy matching conditions are formulated in this context. The first condition describes the thermodynamic driving force behind SF. In this regard, the energy of S<sub>1</sub> must be greater than twice the energy of T<sub>1</sub>, i.e.,  $E(S_1) > 2E(T_1)$ . The second requirement serves to prevent competing deactivation processes such as triplet-triplet annihilation (TTA). Consequently, the energy of the higher triplet state T<sub>2</sub> must be at least two times the energy of T<sub>1</sub>, i.e.,  $E(T_2) > 2E(T_1)$ .<sup>[2,4]</sup> The efficiency of SF is also influenced by the nature and strength of interchromophoric interactions, with strong electronic coupling resulting in fast SF processes.<sup>[2,5]</sup> Thus, the design of the chromophores is crucial for SF. Among the most important properties, SF chromophores should possess high triplet quantum yields, singlet excited state energies of  $\approx 2.2 \text{ eV}$ , and long fluorescence lifetimes.<sup>[2]</sup> Acene derivatives, especially pentacene (Pnc), have been frequently used as models for the study of the photophysical processes behind SF, since their excited states fulfill the energy requirements.<sup>[2,6]</sup> In order to improve both solubility and stability, the Pnc framework is often functionalized with trialkylsilyl ethynyl groups.<sup>[7,8]</sup> Pentacene covalent dimers (Pnc<sub>2</sub>) have been extensively investigated as prototypical systems for the study of intramolecular SF (i-SF) in dilute solution.<sup>[6,9,10]</sup> In these systems, the distance, geometry, and electronic coupling of the interacting chromophores can be specifically controlled by tailoring the spacer groups. In particular, *meta*-functionalized phenylenes have been shown to favor through-bond electronic coupling despite a cross-conjugated electronic  $\pi$ -system.<sup>[6]</sup>

Various porphyrinoids have been investigated as energy-donor antennas to widen the spectral range for activation of SF.<sup>[11–14]</sup> Nevertheless, these chromophores feature drawbacks that relate


A.-S. Wollny, I. Papadopoulos, D. M. Guldi  
Department of Chemistry and Pharmacy  
Friedrich-Alexander-University Erlangen-Nürnberg  
Egerlandstraße 3, 91058 Erlangen, Germany  
E-mail: dirk.guldi@fau.de

G. Lavarda, I. López-Duarte, T. Torres  
Department of Organic Chemistry and Institute for Advanced Research in Chemical Sciences (IAdChem)  
Universidad Autónoma de Madrid  
Cantoblanco, Madrid 28049, Spain  
E-mail: tomas.torres@uam.es

H. Gotfredsen, Y. Hou, R. R. Tykwinski  
Department of Chemistry  
University of Alberta  
11227 Saskatchewan Drive, Edmonton, Alberta T6G 2G2, Canada  
E-mail: tykwinsk@ualberta.ca

H. Gotfredsen  
Department of Chemistry  
University of Copenhagen  
Universitetsparken 5, Copenhagen Ø 2100, Denmark

T. Torres  
IMDEA-Nanociencia  
c/Faraday 9, Cantoblanco, Madrid 28049, Spain

 The ORCID identification number(s) for the author(s) of this article can be found under <https://doi.org/10.1002/adom.202300500>

© 2023 The Authors. Advanced Optical Materials published by Wiley-VCH GmbH. This is an open access article under the terms of the Creative Commons Attribution License, which permits use, distribution and reproduction in any medium, provided the original work is properly cited.

DOI: 10.1002/adom.202300500

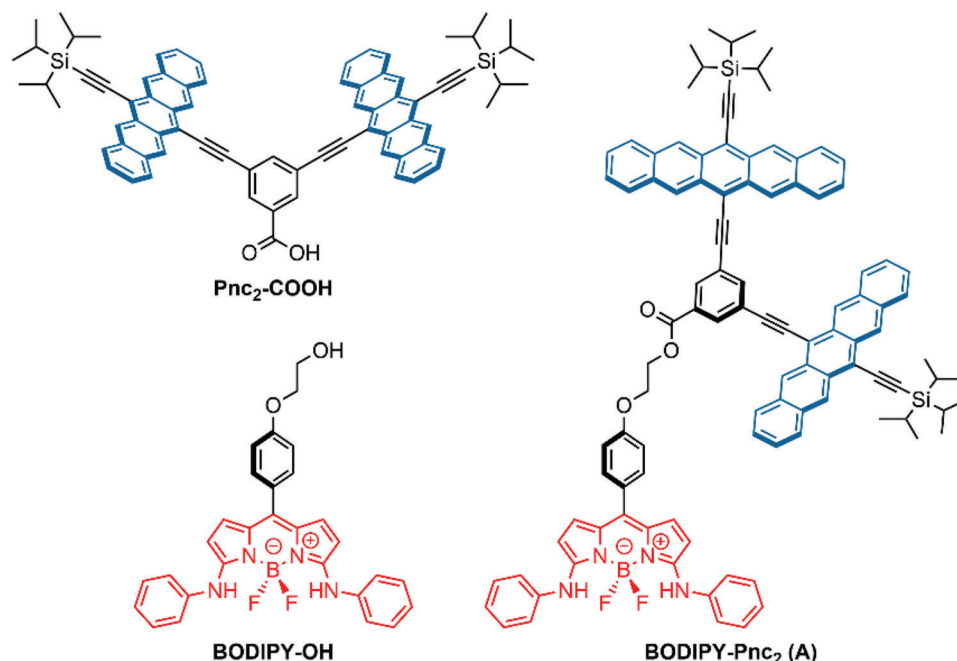


**Figure 1.** Chemical structure of **BODIPY-Pnc<sub>2</sub> A** together with the reference compounds **BODIPY-OH** and **Pnc<sub>2</sub>-COOH**.

to their limited photo-stability and versatility toward chemical modification.<sup>[15]</sup> Boron-dipyrromethene (BODIPY) is a versatile molecular building block that has not yet been exploited to enable SF. In addition to its remarkable photo- and chemical stability, BODIPY and its derivatives bring several attractive features as light harvesting energy donors.<sup>[16–18]</sup> As a matter of fact, these chromophores feature large extinction coefficients and high emission quantum yields. Moreover, the absorption and fluorescence properties can be finely tuned by targeted synthetic design. BODIPYs generally feature sharp absorption bands that complement the absorption of pentacene dimers, which would contribute to a strong, nearly panchromatic absorption across the visible range of the solar spectrum. Furthermore, a tailored functionalization of the BODIPY core would ensure a good overlap between BODIPY emission and pentacene absorption, which is an important prerequisite for efficient Förster Resonance Energy Transfer (FRET).

In this paper, we report on the unprecedented activation of intramolecular SF via intramolecular FRET (*i*-FRET) using BODIPY as an energy donor in **BODIPY-Pnc<sub>2</sub>** covalent conjugate **A**. In addition, the influence of solvent polarity is investigated by comparing the photophysical behavior in toluene and benzonitrile. By combining steady-state and transient spectroscopic techniques, an overall picture of the deactivation process emerges, which shows an effective energy transfer and its influence on the efficiency of SF.

## 2. Results

The design of **BODIPY-Pnc<sub>2</sub> A** was aimed at ensuring a strong absorption throughout large part of the visible spectrum along with an efficient FRET from the BODIPY to the Pnc<sub>2</sub> chromophore. In particular, to boost the emission and guarantee its

complementarity with Pnc absorption, the BODIPY core was decorated at the 3- and 5-positions with aniline fragments, which are known to have a significant effect on the optical properties of boron-dipyrromethene chromophores.<sup>[18]</sup> As a matter of fact, the introduction of two aniline substituents results in a significant bathochromic shift of both the absorption and the emission bands, as well as in a sharp increase of the fluorescence quantum yields.<sup>[18]</sup> On the other hand, the Pnc<sub>2</sub> fragment was attached through an alkyl linker to the *meso* position of the BODIPY structure to guarantee flexibility and prevent through-bond coupling (Figure 1).

Steady-state absorption spectroscopy was used to explore possible ground-state interactions between the BODIPY and Pnc<sub>2</sub> chromophores in **A**. Figure 2a depicts the steady-state absorption spectra of **Pnc<sub>2</sub>-COOH**, **BODIPY-OH**, and **A** in toluene. **Pnc<sub>2</sub>-COOH** exhibits the characteristic fine-structured long-wavelength absorption between 500 and 700 nm.<sup>[19]</sup> On the other hand, the absorption spectrum of **BODIPY-OH** is strongly red-shifted in comparison to the typical absorption features of BODIPY chromophores, with an intense maximum located at 597 nm. In qualitative terms, the absorption features of **A** are the superposition of the individual chromophoric components. In comparison to **A**, the individual extinction coefficients of **BODIPY-OH** are lower and those of **Pnc<sub>2</sub>-COOH** are higher, which indicates some level of ground-state interactions between the individual components.

Next, we turned to steady-state fluorescence measurements to shed light onto interactions in the excited states (Figure 2b). Using a photo-excitation wavelength of 610 nm, **Pnc<sub>2</sub>-COOH** reveals a fluorescence band with maximum at 665 nm in toluene, which corresponds to a Stokes shift of 6 nm. The corresponding fluorescence quantum yield ( $\Phi_f$ ) is 2%. On the other hand, the emission spectrum of **BODIPY-OH** recorded upon photo-excitation

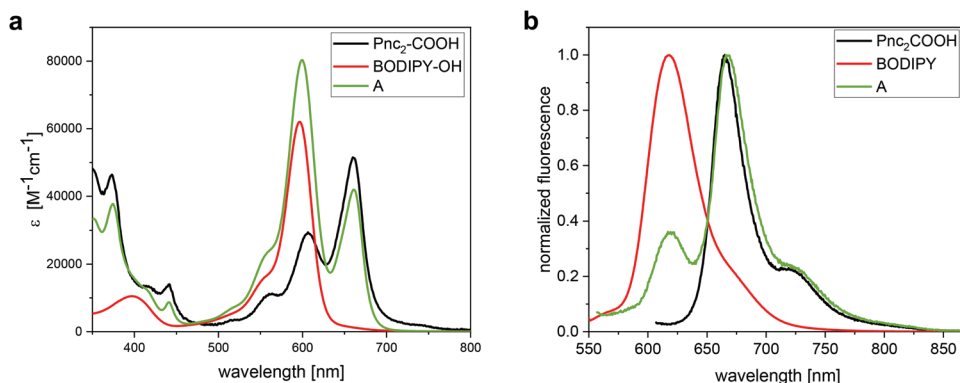


**Figure 2.** a) Steady state absorption spectra of **Pnc<sub>2</sub>-COOH** (black), **BODIPY-OH** (red), and **A** (green) in toluene. b) Normalized fluorescence spectra of **Pnc<sub>2</sub>-COOH** (black), **BODIPY-OH** (red), and **A** (green) in toluene.

**Table 1.** Steady state absorption and fluorescence properties next to TCSPC lifetimes of **BODIPY-OH**, **Pnc<sub>2</sub>COOH** and **A** in toluene.

Compound	$\lambda_{\text{abs}}$ [nm]		$\lambda_{\text{em}}$ [nm]		Stokes shift		$\Phi_F$ [%]	$\tau_{\text{TCSPC}}$ [ns]	
	BODIPY	Pnc <sub>2</sub>	BODIPY	Pnc <sub>2</sub>	BODIPY	Pnc <sub>2</sub>		BODIPY	Pnc <sub>2</sub>
<b>BODIPY-OH</b>	597	—	618	—	21	—	82	3.8	—
<b>Pnc<sub>2</sub>-COOH</b>	—	660	—	665	—	5	2	—	<0.2 <sup>a)</sup>
<b>A</b>	600	661	619	666	19	5	0.2	—	<0.2 <sup>a)</sup>

<sup>a)</sup> The lifetime is below the resolution limit of the TCSPC setup, that is, 200 ps.

at 540 nm in toluene maximizes at 618 nm, which results in a Stokes shift of 21 nm, and a  $\Phi_F = 82\%$ . In the emission spectrum of **A**, the fluorescence features of both **BODIPY** and **Pnc<sub>2</sub>** are discernable. Importantly, the fluorescence arising from **BODIPY** is clearly quenched with  $\Phi_F = 0.2\%$ . This constitutes a strong indication for *i*-FRET, in which the singlet energy of the photo-excited **BODIPY** is transferred to the **Pnc<sub>2</sub>** chromophore. The appearance of an intense **Pnc<sub>2</sub>**-centered fluorescence after **BODIPY**-centered photoexcitation corroborates the occurrence of *i*-FRET in **A**.

In addition to the steady state fluorescence spectra, 3D fluorescence heat maps were recorded and provided further evidence for the energy transfer (Figure S10, Supporting Information). Additional support for *i*-FRET was derived from the fluorescence excitation spectrum of **A**, which matches the absorption spectrum of the **BODIPY** chromophore (Figure S8, Supporting Information).

Independent confirmation of *i*-FRET is provided by time-correlated single photon counting (TCSPC) measurements (Figure S12 and Table S4, Supporting Information). For **BODIPY-OH**, the fluorescence lifetime ( $\tau_{\text{TCSPC}}$ ) is as long as 3.8 ns. In contrast, **BODIPY**-centered photoexcitation in **A** leads to a  $\tau_{\text{TCSPC}}$  of <0.2 ns. In other words, *i*-FRET appears to occur on a sub-ns timescale. On the other hand, upon pentacene-centered photo-excitation of either **Pnc<sub>2</sub>-COOH** or **A**,  $\tau_{\text{TCSPC}}$  values shorter than the resolution limit of the TCSPC setup are obtained. This is consistent with the occurrence of *i*-SF at **Pnc<sub>2</sub>**. An overview of the steady-state absorption and fluorescence measurements together with the  $\tau_{\text{TCSPC}}$  values in toluene is reported in Table 1.

When performing steady-state measurements in the more polar solvent benzonitrile, only minor differences are noted in comparison to toluene. The absorption maxima of **Pnc<sub>2</sub>COOH** ap-

pears to be slightly red-shifted (Figure S7 and Table S2, Supporting Information). For **BODIPY-OH**, a small bathochromic shift of the absorption features is also visible, along with a decrease of  $\Phi_F$  to 65%. The absorption maxima for **A** are slightly red-shifted in benzonitrile as well, which matches the observations made with **BODIPY-OH** and **Pnc<sub>2</sub>COOH**. In the more polar solvent, FRET from the **BODIPY** to the **Pnc<sub>2</sub>** fragment is still operative, as shown by steady-state emission and excitation assays as well as by TCSPC measurements (Figures S9, S11, and S13, and Table S4, Supporting Information).

At this point, femtosecond (fs-TAS) and nanosecond (ns-TAS) transient absorption spectroscopies were performed to clarify details about the kinetics and mechanism of excited state deactivation. Photoexcitation of **BODIPY-OH** and **A** was carried out at 532 nm, whereas for **Pnc<sub>2</sub>COOH** an excitation wavelength of 632 nm was used. A three species kinetic model to fit the raw data for **Pnc<sub>2</sub>COOH** is well established and also applied in this work (Figures S14, S15, S20, and S21, Supporting Information).<sup>[11–14]</sup> The maxima of the first singlet excited state  $^1(S_1S_0)_{\text{Pnc}_2}$  are found in the visible range at 451 and 510 nm and at 1386 nm in the near-infrared (NIR), along with a shoulder at 570 nm. Ground-state bleaching (GSB) covers a wavelength range from  $\approx 600$  to 670 nm. As the first singlet excited state decays, the triplet signatures emerge with maxima at 447 and 506 nm in the visible region, as well as maxima at 896 and 983 nm in the NIR. Hand-in-hand with the latter is an intensification of the GSB between 600 to 670 nm. This transition, that is, from  $^1(S_1S_0)_{\text{Pnc}_2}$  to the singlet correlated triplet pair state  $^1(T_1T_1)_{\text{Pnc}_2}$ , proceeds via an intermediate species. The species has variable combinations of charge transfer (CT),  $^1(S_1S_0)_{\text{Pnc}_2}$ , and  $^1(T_1T_1)_{\text{Pnc}_2}$  character depending on the solvent. In toluene, for example, the features of  $^1(S_1S_0)_{\text{Pnc}_2}$

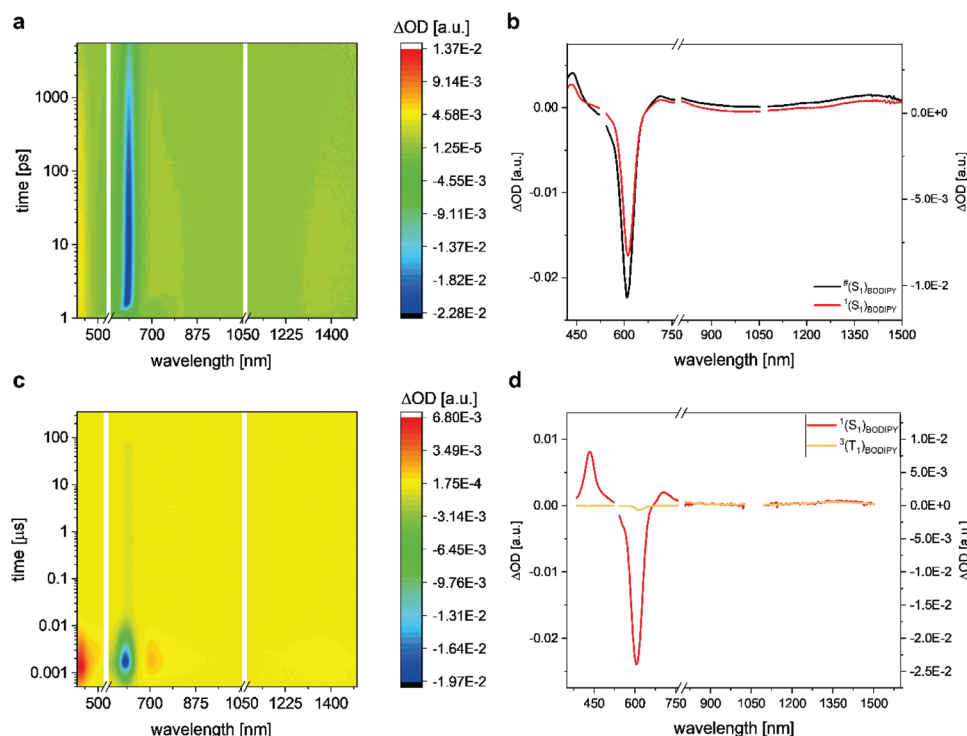


**Figure 3.** a) 3D fluorescence heat map of **BODIPY-OH** obtained by fs-TAS measurements with time delays between 2.3–5500 ps in toluene. b) Evolution associated spectra of the fs-TA data of **BODIPY-OH** in toluene, with the initially formed excited state  $^{\#}(S_1)_{\text{BODIPY}}$  (black) and the first singlet excited state  $^1(S_1)_{\text{BODIPY}}$  (red). c) 3D fluorescence heat map of **BODIPY-OH** obtained by ns-TAS measurements with time delays between 0 and 356  $\mu\text{s}$  in toluene. d) Evolution associated spectra of the ns-TA data of **BODIPY-OH**, with the first singlet excited state  $^1(S_1)_{\text{BODIPY}}$  (red) and the triplet excited state  $^3(T_1)_{\text{BODIPY}}$  (yellow).

are clearly discernable and dominate, while in benzonitrile the  $^1(T_1T_1)_{\text{Pnc2}}$  features are particularly strong. The polarity of the solvent, thus, influences the nature of the intermediate state.

For **BODIPY-OH**, a kinetic model consisting of three species is appropriate as well (Figure 3 and Figures S16, S17, S22, and S23, Supporting Information). The initial state, namely  $^{\#}(S_1)_{\text{BODIPY}}$ , with a lifetime of 151 ps as determined by global analysis of the fs-TAS data, is believed to deactivate via relaxation and/or structural reorientation. This premise is supported by the extremely short lifetime of  $^{\#}(S_1)_{\text{BODIPY}}$ , as well as the matching of the peaks with  $^1(S_1)_{\text{BODIPY}}$ . Following the decay of  $^{\#}(S_1)_{\text{BODIPY}}$ , the first singlet excited state  $^1(S_1)_{\text{BODIPY}}$  is formed, which features a strong maximum at 432 nm, a weaker maximum between 700 and 750 nm, and GSB at  $\approx 612$  nm. For  $^1(S_1)_{\text{BODIPY}}$ , the lifetime derived from the transient absorption measurements (i.e., 3.8 ns) nicely matches the data obtained from TCSPC. Finally, the triplet excited state  $^3(T_1)_{\text{BODIPY}}$  is populated by means of intersystem crossing.

Based on comparisons with the two reference compounds (**BODIPY-OH** and **Pnc<sub>2</sub>COOH**), a kinetic model was developed for **A**, which is based on four species (Figure 4 and Figures S18, S19, S24, and S25, Supporting Information). First,  $^1(S_1)_{\text{BODIPY}}$  of the BODIPY fragment is populated. The spectral characteristics of  $^1(S_1)_{\text{BODIPY}}$  include an intense GSB between 580 and 615 nm in addition to a maximum at 450 nm. For **A**, the state  $^1(S_1)_{\text{BODIPY}}$  decays within 1.8 ps, which is much faster than observed in the reference compound **BODIPY-OH** (3.8 ns). The nature of this

fast deactivation is unidirectional *i*-FRET, in which the excited state energy is transferred from the **BODIPY** to the **Pnc<sub>2</sub>** chromophores. In the NIR region, the signal at  $\approx 1376$  nm corresponds to the first singlet excited state  $^1(S_1)_{\text{BODIPY}}$  of **BODIPY**, and the absence of this signal in the measurements of **BODIPY-OH** is ascribed to its very short lifetime. As such, singlet excited state  $^1(S_1)_{\text{BODIPY}}$  mixes with the strong signal of the first singlet excited state of **Pnc<sub>2</sub>**  $^1(S_1S_0)_{\text{Pnc2}}$ . The *i*-FRET gives rise to  $^1(S_1S_0)_{\text{Pnc2}}$ , whose decay follows the same deactivation cascade as documented for the reference compound **Pnc<sub>2</sub>COOH**. In particular, the characteristic  $^1(S_1S_0)_{\text{Pnc2}}$  maxima of at 450, 510, and 1375 nm afford  $^1(T_1T_1)_{\text{Pnc2}}$  within a timescale of  $>200$  ps. A short-lived intermediate, with variable charge transfer (CT),  $^1(S_1S_0)_{\text{Pnc2}}$ , and  $^1(T_1T_1)_{\text{Pnc2}}$  character, facilitates this transformation as a basis for *i*-SF. Ultimately, the ground state is recovered by intramolecular TTA. Table 2 summarizes the kinetic data for **BODIPY-OH**, **Pnc<sub>2</sub>COOH**, and **A** in toluene.

In addition, triplet-triplet sensitization experiments were performed using *N*-methylfulleropyrrolidine (*N*-MFP) as a triplet sensitizer to identify characteristic pentacene triplet excited state signatures without the influence of external factors (Figure S26, Supporting Information). Due to its high triplet excited state energy, *N*-MFP is subject to a triplet-triplet energy transfer to pentacens. Using a photoexcitation wavelength of 387 nm, *N*-MFP is nearly exclusively photoexcited. To investigate only the pure triplet excited state of the pentacene, the conjugates were not measured to avoid interference.

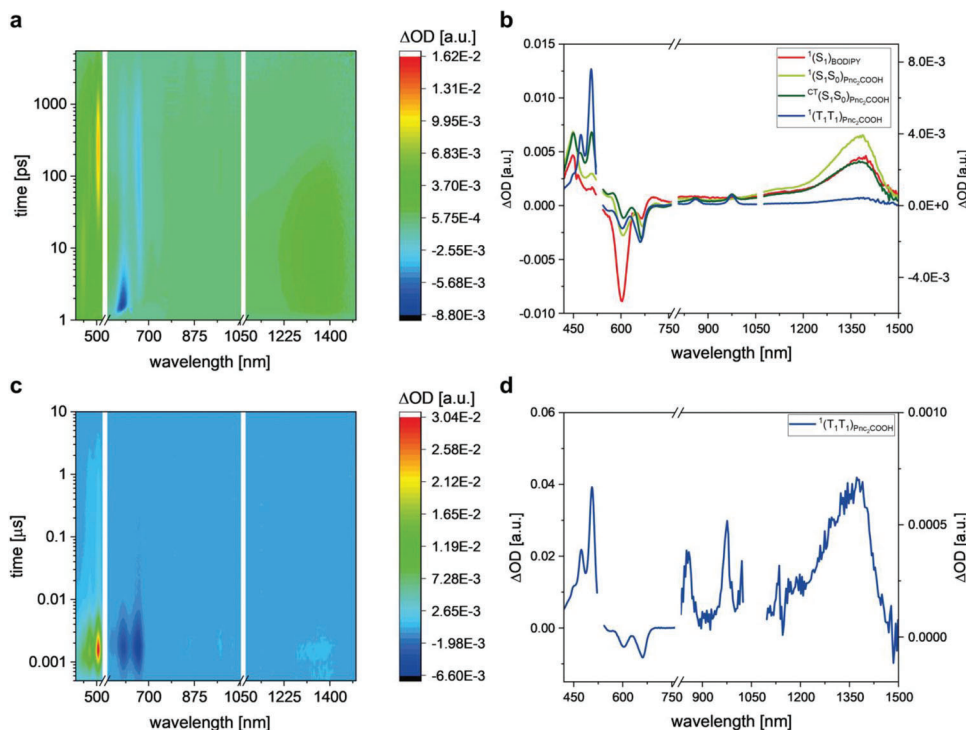


**Figure 4.** a) 3D heat map of **A** obtained by fs-TAS measurements with time delays between 2.3 and 5500 ps in toluene. b) Evolution associated spectra of the fs-TA data of **A** in toluene, with the initially formed **BODIPY** singlet excited state  $^1(S_1)_{\text{BODIPY}}$  (red), the **Pnc<sub>2</sub>** singlet excited state  $^1(S_1S_0)_{\text{Pnc}_2}$  (light green), the intermediate state  $^{\text{CT}}(S_1S_0)_{\text{Pnc}_2}$  (dark green), and singlet correlated triplet pair  $^1(T_1T_1)_{\text{Pnc}_2}$  (blue). c) 3D heat map of **A** obtained by ns-TAS measurements with time delays between 0 and 356  $\mu\text{s}$  in toluene. d) Evolution associated spectra of the ns-TA data of **A** shown in (c), with singlet correlated triplet pair  $^1(T_1T_1)_{\text{Pnc}_2}$  (blue).

**Table 2.** Summary of the lifetimes and triplet quantum yield from transient absorption spectroscopy of **BODIPY-OH**, **Pnc<sub>2</sub>COOH** and **A** in toluene.

Compounds	fs-TAS					ns-TAS		$\Phi_T$ [%]
	$^1(S_1)$	$^1(S_1)$	$^1(S_1S_0)$	$^{\text{CT}}(S_1S_0)$	$^1(T_1T_1)$	$^1(S_1)$	$^1(T_1T_1)$	
	BODIPY	BODIPY	Pnc <sub>2</sub>	Pnc <sub>2</sub>	Pnc <sub>2</sub>	BODIPY	Pnc <sub>2</sub>	
<b>Pnc<sub>2</sub>-COOH</b>	–	–	8.3 ps	76.2 ps	3.3 ns <sup>a)</sup>	–	3.5 ns	120% $\pm$ 20%
<b>BODIPY-OH</b>	151.4 ps	7.4 ns <sup>a)</sup>	–	–	–	3.8 ns	–	–
<b>A</b>	–	1.8 ps	11.6 ps	79.7 ps	2.4 ns <sup>a)</sup>	–	2.5 ns	176% $\pm$ 20%

<sup>a)</sup> The lifetime is too long to be resolved with fs-TAS

When comparing the results of the transient absorption measurements in toluene and benzonitrile, it is noticeable that a higher theoretical *i*-FRET rate, namely  $k_{\text{FRET}} = 7.46 \times 10^{11} \text{ s}^{-1}$ , is obtained in the more polar solvent benzonitrile versus  $5.43 \times 10^{11} \text{ s}^{-1}$  in toluene (Table 3). This tendency is also evident in the lifetimes of  $^1(S_1)_{\text{BODIPY}}$  in **A**. The latter is 1.84 ps in toluene, which is 1.3 times longer than the corresponding value in benzonitrile. On the other hand, the triplet quantum yield (TQY) for **A** increases with increasing solvent polarity from 176% (toluene) to 207% (benzonitrile). It is also noted that the TQY of **A** is significantly higher than that of **Pnc<sub>2</sub>COOH**. Thus, the enhanced TQY might be related to the funneling of high energy photons onto the pentacene dimer, which, in turn, accelerates the overall population of  $^1(T_1T_1)$  with respect to pentacene dimer alone under red-light photoexcitation. A comparison of **A**, that is,

**BODIPYPnc<sub>2</sub>**, with similar systems including subporphyrzine conjugates and subphthalocyanine-pentacene conjugates, with rates of  $k_{\text{FRET}} = 1.14$  and  $4.09 \times 10^{11} \text{ s}^{-1}$ , respectively, in benzonitrile, demonstrates that **A** exhibits a similar or even more efficient FRET.<sup>[11,14,20]</sup>

### 3. Conclusion

In summary, we have documented that *i*-FRET enables in **A** transduction of singlet excited state energy from BODIPY to Pnc<sub>2</sub>. The latter is in a subsequent step subject to *i*-SF. A more polar solvent favors a faster *i*-FRET with rates as high as  $7.46 \times 10^{11} \text{ s}^{-1}$  and a more efficient *i*-SF with a TQY as high as 207%  $\pm$  20% in benzonitrile. As mentioned above, the decay from the singlet correlated triplet pair  $^1(T_1T_1)_{\text{Pnc}_2}$  undergoes mainly intramolec-



**Table 3.** Summary of the parameters used to calculate FRET rate constants of **A** in toluene and benzonitrile.

	$\tau_{DA}^a)$ [ps]	$\tau_D^b)$ [ns]	$\epsilon_{Max}^c)$ [M <sup>-1</sup> cm <sup>-1</sup> ]	$\Phi_F^d)$	$J$ [M <sup>-1</sup> cm <sup>-1</sup> nm <sup>4</sup> ) <sup>e)</sup>	$R_0$ [Å] <sup>f)</sup>	$R$ [Å] <sup>g)</sup>	$k_{FRET}^h)$ [10 <sup>11</sup> s <sup>-1</sup> ] <sup>h)</sup>	$E_{FRET}^i)$
<b>A</b> in toluene	1.84	3.77	42000	0.82	$2.92 \times 10^{15}$	55.24	15.5	5.43	0.9995
<b>A</b> in benzonitrile	1.43	3.76	30000	0.65	$2.22 \times 10^{15}$	49.87	13.28	7.46	0.9996

<sup>a)</sup> Lifetime of the energy donor in the presence of the energy acceptor from the Global Analysis of fs-TAS; <sup>b)</sup> Energy donor lifetime from the TCSPC measurements; <sup>c)</sup> Maximum extinction coefficient of the pentacene component; <sup>d)</sup>  $\Phi_F$  Energy Donor; <sup>e)</sup> Degree of spectral overlap; <sup>f)</sup> Energy donor-acceptor distance; <sup>g)</sup> FRET distance; <sup>h)</sup> FRET rate constant; <sup>i)</sup> Efficiency of FRET. The derivations are displayed in the SI.

ular TTA. As a matter of fact, the triplets cannot diffuse apart as they are confined to the pentacene units. In turn, the uncorrelated triplet pair is formed in only negligible amounts and is omitted from the deactivation cascade. Although triplet formation is not noted, the overall concept of funneling energy from different parts of the visible solar spectrum onto a pentacene dimer in order to trigger SF opens up new design guidelines for future systems.

## 4. Experimental Section

Conjugate **A** was synthesized by esterification using precursors **BODIPY-OH** and **Pnc<sub>2</sub>-COOH**. The synthetic procedures, along with the characterization of the synthesized products, are reported in the Supporting Information.

Steady state absorption experiments were performed on a Perkin Elmer Lambda 2 UV/Vis double beam spectrometer. Steady state emission experiments were performed on the Horiba Jobin Yvon FluoroMax-3 fluorometer and an FS5 Spectrofluorometer (Edinburgh Instruments). Zinc 2,9,16,23-tetra-*tert*-butyl-29H,31H-phthalocyanine (FQY = 0.3 in Tol), cresyl violet (FQY = 0.56 in ethanol) and Rhodamine 6G (FQY = 0.95 in ethanol) were used as references to determine the fluorescence quantum yield of the pentacene and BODIPY centered fluorescence.<sup>[21,22]</sup>

For the TCSPC measurements, the TemPro system from HORIBA Jobin Yvon was used in combination with a TBX picosecond photon detection module. The evaluation of the data was performed with the DAS 6 software from Horiba.

For the fs-TAS measurements, a HELIOS “transient absorption pump-probe system” (TAPPS) detection unit from Ultrafast systems was used, in combination with a Ti:sapphire laser system CPA-2101 (Clark-MXR Inc.). The wavelengths used were 532 and 632 nm and were adjusted with a noncollinear optical parametric amplifier (NOPA, Clark MXR.). For the ns-TAS experiments an EOS TAPPS detection unit from Ultrafast systems was used.

## Supporting Information

Supporting Information is available from the Wiley Online Library or from the author.

## Acknowledgements

A.-S.W., G.L., and I.P. contributed equally to this work. D.M.G. thanks the financial support from “the German Research Foundation (DFG) via SFB 953 “Synthetic Carbon Allotropes” and “Solar Technologies go Hybrid (SolTech)” Initiative of the Bavarian Ministry for Science. T.T. acknowledges financial support from MICINN (PID2020-116490GB-I00 and TED2021-131255B-C43), the Comunidad de Madrid and the Spanish State through the Recovery, Transformation and Resilience Plan [“Materiales Disruptivos Bidimensionales (2D)” (MAD2D-CM) (UAM1)-MRR Materiales Avanzados], and the European Union through the Next Generation

EU funds. IMDEA Nanociencia acknowledges support from the “Severo Ochoa” Programme for Centres of Excellence in R&D (MINECO, Grant SEV2016-0686). R.R.T. acknowledges funding from the Natural Sciences and Engineering Research Council of Canada (NSERC, grant no. RGPIN-2017-05052) and the Canada Foundation for Innovation (CFI).

## Conflict of Interest

The authors declare no conflict of interest.

## Data Availability Statement

The data that support the findings of this study are available from the corresponding author upon reasonable request.

## Keywords

BODIPY, down conversion, energy transfer, pentacene, photoenergy conversion, singlet fission, time-resolved spectroscopy

Received: February 28, 2023

Revised: April 25, 2023

Published online:

- [1] J. Mohtasham, *Energy Procedia* **2015**, 74, 1289.
- [2] M. B. Smith, J. Michl, *Annu. Rev. Phys. Chem.* **2013**, 64, 361.
- [3] M. C. Hanna, A. J. Nozik, *J. Appl. Phys.* **2006**, 100, 074510.
- [4] R. Casillas, I. Papadopoulos, T. Ullrich, D. Thiel, A. Kunzmann, D. M. Guldi, *Energy Environ. Sci.* **2020**, 13, 2741.
- [5] M. B. Smith, J. Michl, *Chem. Rev.* **2010**, 110, 6891.
- [6] J. Zirzmeier, D. Lehnher, P. B. Coto, E. T. Chernick, R. Casillas, B. S. Basel, M. Thoss, R. R. Tykwinski, D. M. Guldi, *Proc. Natl. Acad. Sci. USA* **2015**, 112, 5325.
- [7] D. J. Gundlach, J. E. Royer, S. K. Park, S. Subramanian, O. D. Jurchescu, B. H. Hamadani, A. J. Moad, R. J. Kline, L. C. Teague, O. Kirillov, C. A. Richter, J. G. Kushmerick, L. J. Richter, S. R. Parkin, T. N. Jackson, J. E. Anthony, *Nat. Mater.* **2008**, 7, 216.
- [8] B. J. Walker, A. J. Musser, D. Beljonne, R. H. Friend, *Nat. Chem.* **2013**, 5, 1019.
- [9] C. Hetzer, D. M. Guldi, R. R. Tykwinski, *Chem. - Eur. J.* **2018**, 24, 8245.
- [10] R. M. Young, M. R. Wasielewski, *Acc. Chem. Res.* **2020**, 53, 1957.
- [11] D. Guzmán, I. Papadopoulos, G. Lavarda, P. R. Rami, R. R. Tykwinski, M. S. Rodríguez-Morgade, D. M. Guldi, T. Torres, *Angew. Chem., Int. Ed.* **2021**, 60, 1474; *Angew. Chem.* **2021**, 133, 1496.
- [12] J. Zirzmeier, G. Lavarda, H. Gotfredsen, I. Papadopoulos, L. Chen, T. Clark, R. R. Tykwinski, T. Torres, D. M. Guldi, *Nanoscale* **2020**, 12, 23061.

- [13] D.-P. Medina, I. Papadopoulos, G. Lavarda, H. Gotfredsen, P. R. Rami, R. R. Tykwinski, M. S. Rodríguez-Morgade, D. M. Guldi, T. Torres, *Nanoscale* **2019**, *11*, 22286.
- [14] G. Lavarda, J. Zirzmeier, M. Gruber, P. R. Rami, R. R. Tykwinski, T. Torres, D. M. Guldi, *Angew. Chem., Int. Ed.* **2018**, *57*, 16291; *Angew. Chem.* **2018**, *130*, 16528.
- [15] G. Lavarda, J. Labella, M. V. Martínez-Díaz, M. S. Rodríguez-Morgade, A. Osuka, T. Torres, *Chem. Soc. Rev.* **2022**, *51*, 9482.
- [16] R. Ziessel, G. Ulrich, A. Harriman, *New J. Chem.* **2007**, *31*, 496.
- [17] E. Bassan, A. Gualandi, P. G. Cozzi, P. Ceroni, *Chem. Sci.* **2021**, *12*, 6607.
- [18] A. Loudet, K. Burgess, *Chem. Rev.* **2007**, *107*, 4891.
- [19] A. Kunzmann, M. Gruber, R. Casillas, J. Zirzmeier, M. Stanzel, W. Peukert, R. R. Tykwinski, D. M. Guldi, *Angew. Chem., Int. Ed.* **2018**, *57*, 10742; *Angew. Chem.* **2018**, *130*, 10902.
- [20] A summary of previously reported sensitizers is provided in Table S7 (Supporting Information).
- [21] S. L. Murov, I. Carmichael, G. L. Hug, *Handbook of Photochemistry*, Marcel Dekker, New York **1993**.
- [22] A. M. Brouwer, *Pure Appl. Chem.* **2011**, *83*, 2213.